We are IntechOpen, the world's leading publisher of Open Access books Built by scientists, for scientists

4,800
Open access books available

122,000
International authors and editors

135M
Downloads

Our authors are among the

154
Countries delivered to

TOP 1%
most cited scientists

12.2%
Contributors from top 500 universities

CLARIVATE ANALYTICS BOOK CITATION INDEX INDEXED

WEB OF SCIENCE™

Selection of our books indexed in the Book Citation Index in Web of Science™ Core Collection (BKCI)

Interested in publishing with us?
Contact book.department@intechopen.com

Numbers displayed above are based on latest data collected.
For more information visit www.intechopen.com

18

Computational Modeling, Visualization, and Control of 2-D and 3-D Grasping under Rolling Contacts

Suguru Arimoto[1,2], Morio Yoshida[2], and Masahiro Sekimoto[1]
[1]*Ritsumeikan University and* [2]*RIKEN-TRI Collaboration Center*
Japan

Abstract
This chapter presents a computational methodology for modeling 2-dimensional grasping of a 2-D object by a pair of multi-joint robot fingers under rolling contact constraints. Rolling contact constraints are expressed in a geometric interpretation of motion expressed with the aid of arclength parameters of the fingertips and object contours with an arbitrary geometry. Motions of grasping and object manipulation are expressed by orbits that are a solution to the Euler-Lagrange equation of motion of the fingers/object system together with a set of first-order differential equations that update arclength parameters. This methodology is then extended to mathematical modeling of 3-dimensional grasping of an object with an arbitrary shape.
Based upon the mathematical model of 2-D grasping, a computational scheme for construction of numerical simulators of motion under rolling contacts with an arbitrary geometry is presented, together with preliminary simulation results.
The chapter is composed of the following three parts.

Part 1 Modeling and Control of 2-D Grasping under Rolling Contacts between Arbitrary Smooth Contours
Authors: S. Arimoto and M. Yoshida

Part 2 Simulation of 2-D Grasping under Physical Interaction of Rolling between Arbitrary Smooth Contour Curves
Authors: M. Yoshida and S. Arimoto

Part 3 Modeling of 3-D Grasping under Rolling Contacts between Arbitrary Smooth Surfaces
Authors: S. Arimoto, M. Sekimoto, and M. Yoshida

1. Modeling and Control of 2-D Grasping under Rolling Contacts between Arbitrary Smooth Contours

1.1 Introduction

Modeling and control of dynamics of 2-dimensional object grasping by using a pair of multi-joint robot fingers are investigated under rolling contact constraints and an arbitrary geometry of the object and fingertips. First, modeling of rolling motion between 2-D rigid objects with an arbitrary shape is treated under the assumption that the two contour curves coincide at

the contact point and share the same tangent. The rolling contact constraints induce an Euler equation of motion parametrized by a pair of arclength parameters and constrained onto the kernel space as an orthogonal complement to the image space spanned from all the constraint gradients. Further, it is shown that all the Pfaffian forms of the constraints are integrable in the sense of Frobenius and therefore the rolling contacts are regarded as a holonomic constraint. The Euler-Lagrange equation of motion of the overall fingers/object system is derived together with a couple of first-order differential equations that express evolution of contact points in terms of quantities of the second fundamental form. A control signal called “blind grasping" is defined and shown to be effective in stabilization of grasping without using the details of object shape and parameters or external sensing.

1.2 Modeling of 2-D Grasping by Euler-Lagrange Equation

Very recently, a complete model of 2-dimensional grasping of a rigid object with arbitrary shape by a pair of robot fingers with arbitrarily given fingertip shapes (see Fig. 1) is presented based upon the differential-geometric assumptions of rolling contacts [Arimoto et al., 2009a]. The assumptions are summarized as follows:

1) Two contact points on the contour curves must coincide at a single common point without mutual penetration, and

2) the two contours must have the same tangent at the common contact point.

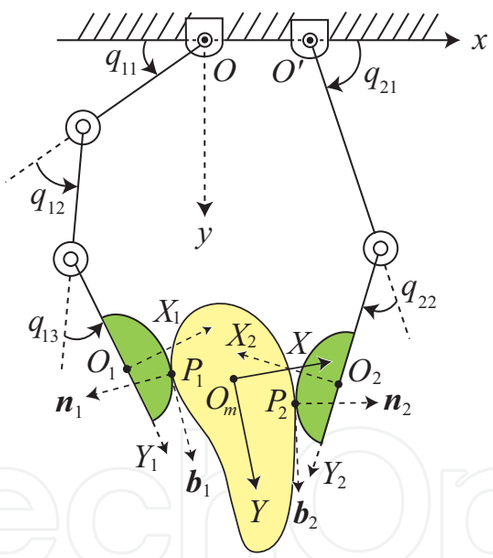

Fig. 1. A pair of two-dimensional robot fingers with a curved fingertip makes rolling contact with a rigid object with a curved contour.

As pointed out in the previous papers [Arimoto et al., 2009a] [Arimoto et al., 2009b], these two conditions as a whole are equivalent to Nomizu’s relation [Nomizu, 1978] concerning tangent vectors at the contact point and normals to the common tangent. As a result, a set of Euler-Lagrange’s equations of motion of the overall fingers/object system is presented in the

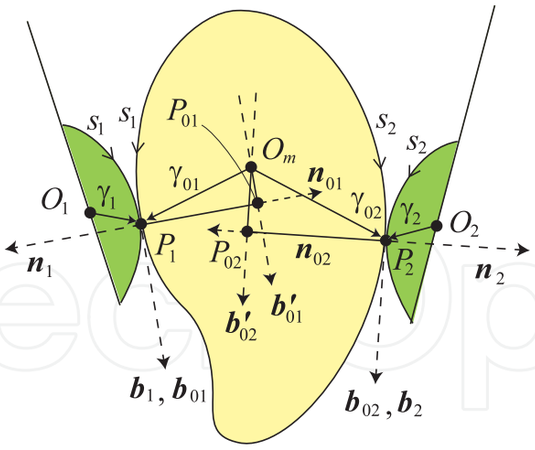

Fig. 2. Definitions of tangent vectors $\boldsymbol{b}_i$, $\boldsymbol{b}_{0i}$ and normals $\boldsymbol{n}_i$ and $\boldsymbol{n}_{0i}$ at contact points P_i for $i = 1, 2$.

following forms:

$$M\ddot{\boldsymbol{x}} - \sum_{i=1,2} (f_i \bar{\boldsymbol{n}}_{0i} + \lambda_i \bar{\boldsymbol{b}}_{0i}) = 0 \tag{1}$$

$$I\ddot{\theta} + \sum_{i=1,2} (-1)^i \{f_i (\boldsymbol{b}_{0i}^{\mathrm{T}} \gamma_{0i}) - \lambda_i (\boldsymbol{n}_{0i}^{\mathrm{T}} \gamma_{0i}) = 0 \tag{2}$$

$$\begin{aligned} G_i(q_i)\ddot{q}_i + \left\{ \frac{1}{2}\dot{G}_i(q_i) + S_i(q_i, \dot{q}_i) \right\} \dot{q}_i + f_i \{ J_i^{\mathrm{T}}(q_i) \bar{\boldsymbol{n}}_{0i} - (-1)^i (\boldsymbol{b}_i^{\mathrm{T}} \gamma_i) \boldsymbol{e}_i \} \\ + \lambda_i \left\{ J_i^{\mathrm{T}}(q_i) \bar{\boldsymbol{b}}_{0i} - (-1)^i (\boldsymbol{n}_i^{\mathrm{T}} \gamma_i) \boldsymbol{e}_i \right\} = u_i, \quad i = 1, 2 \end{aligned} \tag{3}$$

where q_i denotes the joint vector as $q_1 = (q_{11}, q_{12}, q_{13})^{\mathrm{T}}$ and $q_2 = (q_{21}, q_{22})^{\mathrm{T}}$, $\dot{\theta}$ denotes the angular velocity of rotation of the object around the object mass center O_m expressed by position vector $\boldsymbol{x} = (x, y)^{\mathrm{T}}$ in terms of the inertial frame coordinates O-xy. Equation (1) expresses the translational motion of the object with mass M and (2) its rotational motion with inertia moment I around the mass center O_m. At the contact point P_i, $\boldsymbol{b}_i$ denotes the unit tangent vector expressed in local coordinates of O_i-X_iY_i fixed to the fingertip of finger i ($i = 1, 2$) as shown in Fig. 1, and $\boldsymbol{n}_i$ denotes the unit normal to the tangent expressed in terms of O_i-X_iY_i. Similarly, $\boldsymbol{b}_{0i}$ and $\boldsymbol{n}_{0i}$ are the unit tangent and normal at P_i expressed in terms of local coordinates O_m-XY fixed to the object. All these unit vectors are determined uniquely from the assumptions 1) and 2) on the rolling contact constraints at each contact point P_i dependently on each corresponding value s_i of arclength parameter for $i = 1, 2$ as shown in Fig. 2. Equation (3) denotes joint motions of finger i with the inertia matrix $G_i(q_i)$ for $i = 1, 2$ and $\boldsymbol{e}_1 = (1, 1, 1)^{\mathrm{T}}$ and $\boldsymbol{e}_2 = (1, 1)^{\mathrm{T}}$. All position vectors γ_i and γ_{0i} for $i = 1, 2$ are defined as in Fig. 2 and expressed in their corresponding local coordinates, respectively. Both the unit vectors $\bar{\boldsymbol{b}}_{0i}$ and $\bar{\boldsymbol{n}}_{0i}$ are expressed in the inertial frame coordinates as follows:

$$\bar{\boldsymbol{b}}_{0i} = \Pi_0 \boldsymbol{b}_{0i}, \quad \bar{\boldsymbol{n}}_{0i} = \Pi_0 \boldsymbol{n}_{0i}, \quad \Pi_0 = (\boldsymbol{r}_X, \boldsymbol{r}_Y) \tag{4}$$

where $\Pi_0 \in SO(2)$ and $\boldsymbol{r}_X$ and $\boldsymbol{r}_Y$ denote the unit vectors of X- and Y-axes of the object in terms of the frame coordinates O-xy. In the equations of (1) to (3), f_i and λ_i are Lagrange's multipliers that correspond to the following rolling contact constraints respectively:

$$\begin{cases} Q_{bi} = (\boldsymbol{r}_i - \boldsymbol{r}_m)^{\mathrm{T}} \bar{\boldsymbol{b}}_{0i} + \boldsymbol{b}_i^{\mathrm{T}} \gamma_i - \boldsymbol{b}_{0i}^{\mathrm{T}} \gamma_{0i} = 0, \quad i = 1,2 & (5) \\ Q_{ni} = (\boldsymbol{r}_i - \boldsymbol{r}_m)^{\mathrm{T}} \bar{\boldsymbol{n}}_{0i} - \boldsymbol{n}_i^{\mathrm{T}} \gamma_i - \boldsymbol{n}_{0i}^{\mathrm{T}} \gamma_{0i} = 0, \quad i = 1,2 & (6) \end{cases}$$

where $\boldsymbol{r}_i$ denotes the position vector of the fingertip center O_i expressed in terms of the frame coordinates O-xy and $\boldsymbol{r}_m$ the position vector of O_m in terms of O-xy. In parallel with Euler-Lagrange's equations (1) to (3), arclength parameters s_i $(i = 1,2)$ should be governed by the following formulae of the first order differential equation :

$$\{\kappa_{0i}(s_i) + \kappa_i(s_i)\} \frac{\mathrm{d}s_i}{\mathrm{d}t} = (-1)^i (\dot{\theta} - \dot{p}_i), \quad i = 1,2 \tag{7}$$

where $\kappa_i(s_i)$ denotes the curvature of the fingertip contour for $i = 1,2$ and $\kappa_{0i}(s_i)$ the curvature of the object contour at contact point P_i corresponding to length parameter s_i for $i = 1,2$. Throughout the paper we use $\dot{(\cdot)}$ for denoting the differentiation of the content of bracket ( ) in time t as $\dot{\theta} = \mathrm{d}\theta/\mathrm{d}t$ in (7) and $(')$ for that of ( ) in length parameter s_i as illustrated by $\gamma_i'(s_i) = \mathrm{d}\gamma_i(s_i)/\mathrm{d}s_i$. As discussed in the previous papers, we have

$$\boldsymbol{b}_i(s_i) = \gamma_i'(s_i) \left(= \frac{\mathrm{d}\gamma_i(s_i)}{\mathrm{d}s_i} \right), \quad \boldsymbol{b}_{0i}(s_i) = \gamma_{0i}'(s_i), \quad i = 1,2 \tag{8}$$

and

$$\boldsymbol{n}_i(s_i) = \kappa_i(s_i) \boldsymbol{b}_i'(s_i), \quad \boldsymbol{n}_{0i}(s_i) = \boldsymbol{b}_{0i}'(s_i), \quad i = 1,2 \tag{9}$$

and further

$$\boldsymbol{b}_i(s_i) = -\kappa_i(s_i) \boldsymbol{n}_i'(s_i), \quad \boldsymbol{b}_{0i}(s_i) = -\kappa_{0i}(s_i) \boldsymbol{n}_{0i}'(s_i), \quad i = 1,2 \tag{10}$$

It is well known as in text books on differential geometry of curves and surfaces (for example, see [Gray et al., 2006]) that equations (9) and (10) constitute Frenet-Serre's formulae for the fingertip contour curves and object contours. Note that all equations of (1) to (3) are characterized by length parameters s_i for $i = 1,2$ through unit vectors $\boldsymbol{n}_{0i}$, $\boldsymbol{b}_{0i}$, $\boldsymbol{b}_i$, and $\boldsymbol{n}_i$, and vectors γ_{0i} and γ_i expressed in each local coordinates, but quantities of the second fundamental form of contour curves, that is, $\kappa_i(s_i)$ and $\kappa_0(s_i)$ for $i = 1,2$, do not enter into equations (1) to (3). It is shown that the set of Euler-Lagrange equations of motion (1) to (3) can be derived by applying the variational principle to the Lagrangian of the system

$$L(X; s_1, s_2) = K(X, \dot{X}) - \sum_{i=1,2} (f_i Q_{ni} + \lambda_i Q_{bi}) \tag{11}$$

where X denotes the position state vector defined as

$$X = (x, y, \theta, q_1^{\mathrm{T}}, q_2^{\mathrm{T}})^{\mathrm{T}} \tag{12}$$

and

$$K(X, \dot{X}) = \frac{M}{2}(\dot{x}^2 + \dot{y}^2) + \frac{I}{2}\dot{\theta}^2 + \sum_{i=1,2} \frac{1}{2} \dot{q}_i^{\mathrm{T}} G_i(q_i) \dot{q}_i \tag{13}$$

Note that $K(X, \dot{X})$ is independent of the shape parameters s_1 and s_2 but Q_{ni} and Q_{bi} defined by (5) and (6) are dependent on s_i for $i = 1, 2$ respectively. The variational principle is written in the following form:

$$\int_{t_0}^{t_1} \left\{ \delta L + u_1^{\mathrm{T}} \delta q_1 + u_2^{\mathrm{T}} \delta q_2 \right\} \mathrm{d}t = 0 \tag{14}$$

From this it follows that

$$G(X)\ddot{X} + \left(\frac{1}{2}\dot{G}(X) + S(X, \dot{X}) \right) \dot{X} + \sum_{i=1,2} \left(f_i \frac{\partial}{\partial X} Q_{ni} + \lambda_i \frac{\partial}{\partial X} Q_{bi} \right) = B \begin{pmatrix} u_1 \\ u_2 \end{pmatrix} \tag{15}$$

where $G(X) = \mathrm{diag}(M, M, I, G_1(q_1), G_2(q_2))$, $S(X, \dot{X})$ is a skew-symmetric matrix, and B denotes the 8×5 constant matrix defined as $B^{\mathrm{T}} = (0_{3\times5}, I_5)$, $0_{3\times5}$ signifies the 3×5 zero matrix, and I_5 the 5×5 identity matrix.

1.3 Fingers-Thumb Opposable Control Signals

In order to design adequate control signals for a pair of multi-joint fingers like the one shown in Fig. 1, we suppose that the kinematics of both the robot fingers are known and measurement data of joint angles and angular velocities are available in real-time but the geometry of an object to be grasped is unknown and the location of its mass center together with its inclination angle can not be measured or sensed. This supposition is reasonable because the structure of robot fingers is fixed for any object but the object to be grasped is changeable from time to time. This standpoint is coincident to the start point of Riemannian geometry that, if the robot (both the robot fingers) has its own internal world, then the robot kinematics based upon quantities of the first fundamental form like $\gamma_i(s_i)$ and $\boldsymbol{b}_i(s_i)$ together with q_i and $\dot{q}_i$ must be accessible because these data are intrinsic to the robot's internal world. However, any quantities of the second fundamental form like $\kappa_i(s_i)$ $(i = 1, 2)$ can not be determined from the robot's intrinsic world. By the same season, we assume that the positions of finger centers O_1 and O_2 denoted by $\boldsymbol{r}_1$ and $\boldsymbol{r}_2$ are accessible from the intrinsic robot world and further the Jacobian matrices defined by $J_i(q_i) = \partial \boldsymbol{r}_i / \partial q_i$ for $i = 1, 2$ are also assumed to be intrinsic, that is, real-time computable. Thus, let us now consider a class of control signals defined by the following form

$$u_i = -c_i \dot{q}_i + (-1)^i \beta J_i^{\mathrm{T}}(q_i)(\boldsymbol{r}_1 - \boldsymbol{r}_2) - \alpha_i \hat{N}_i \boldsymbol{e}_i, \quad i = 1, 2 \tag{16}$$

where β stands for a position feedback gain common for $i = 1, 2$ with physical unit [N/m], α_i is also a positive constant common for $i = 1, 2$, $\hat{N}_i$ is defined as

$$\hat{N}_i = \boldsymbol{e}_i^{\mathrm{T}} \{ q_i(t) - q_i(0) \} = p_i(t) - p_i(0), \quad i = 1, 2 \tag{17}$$

and c_i denotes a positive constant for joint damping for $i = 1, 2$. The first term of the right hand side of (16) stands for damping shaping, the second term plays a role of fingers-thumb opposition, and the last term adjusts possibly some abundunt motion of rotation of the object through contacts. Note that the sum of inner products of u_i and $\dot{q}_i$ for $i = 1, 2$ is given by the equation

$$\sum_{i=1,2} \dot{q}_i^{\mathrm{T}} u_i = -\frac{\mathrm{d}}{\mathrm{d}t} \left\{ \frac{\beta}{2} \|\boldsymbol{r}_1 - \boldsymbol{r}_2\|^2 + \sum_{i=1,2} \frac{\alpha_i}{2} \hat{N}_i^2 \right\} - \sum_{i=1,2} c_i \|\dot{q}_i\|^2 \tag{18}$$

Substitution of control signals of (16) into (3) yields

$$G_i\ddot{q}_i + \left\{\frac{1}{2}\dot{G}_i + S_i\right\}\dot{q}_i + c_i\dot{q}_i - (-1)^i\beta J_i^{\mathrm{T}}(\boldsymbol{r}_1 - \boldsymbol{r}_2) + \alpha_i\hat{N}_i\boldsymbol{e}_i$$
$$+f_i\left\{J_i^{\mathrm{T}}\bar{\boldsymbol{n}}_{0i} - (-1)^i(\boldsymbol{b}_i^{\mathrm{T}}\gamma_i)\boldsymbol{e}_i\right\} + \lambda_i\left\{J_i^{\mathrm{T}}\bar{\boldsymbol{b}}_{0i} - (-1)^i(\boldsymbol{n}_i^{\mathrm{T}}\gamma_i)\boldsymbol{e}_i\right\} = 0, \quad i = 1,2 \tag{19}$$

Hence, the overall closed-loop dynamics is composed of the set of Euler-Lagrange's equations of (1), (2), and (19) that are subject to four algebraic constraints of (5) and (6) and the pair of the first-order differential equations of (7) that governs the update law of arclength parameters s_1 and s_2. It should be also remarked that, according to (18), the sum of inner products of (1) and $\dot{\boldsymbol{x}}$, (2) and $\dot{\theta}$, and (19) and $\dot{q}_i$ for $i = 1,2$ yields the energy relation

$$\frac{\mathrm{d}}{\mathrm{d}t}E(X,\dot{X}) = -\sum_{i=1,2} c_i\|\dot{q}_i\|^2 \tag{20}$$

where

$$E(X,\dot{X}) = K(X,\dot{X}) + P(X) \tag{21}$$
$$P(X) = \frac{\beta}{2}\|\boldsymbol{r}_1 - \boldsymbol{r}_2\|^2 + \sum_{i=1,2}\frac{\alpha_i}{2}\hat{N}_i^2 \tag{22}$$

and $K(X,\dot{X})$ is the total kinetic energy defined by (13) and $P(X)$ is called the artificial potential energy that is a scalar function depending on only q_1 and q_2. It is important to note that the closed-loop dynamics of (1), (2), and (19) can be written into the general form, correspondingly to (15),

$$G(X)\ddot{X} + \left\{\frac{1}{2}\dot{G}(X) + S(X,\dot{X}) + C\right\}\dot{X} + \frac{\partial P(X)}{\partial X}$$
$$+\sum_{i=1,2}\left(f_i\frac{\partial}{\partial X}Q_{ni} + \lambda_i\frac{\partial}{\partial X}Q_{bi}\right) = 0 \tag{23}$$

where $C = \mathrm{diag}(0_2, 0, c_1 I_3, c_2 I_2)$. This can be also obtained by applying the principle of variation to the Lagrangian

$$L = K(X,\dot{X}) - P(X) - \sum_{i=1,2}(f_i Q_{ni} + \lambda_i Q_{bi}) \tag{24}$$

1.4 Necessary Conditions for Design of Fingertip Shape

It has been known [Arimoto, 2008] that, in a simple case of "ball-plate" pinching, a solution to the closed-loop dynamics corresponding to (23) under some holonomic constraints of rolling contacts converge to a steady (equilibrium) state that minimizes the potential $P(X)$ under the constraints. However, a stabilization problem of control signals like (16) still remains unsolved or rather has not yet been tackled not only in a general setup of arbitrary geometry like the situation shown in Fig. 1 but also in a little more simple case that the object to be grasped is a parallelepiped but the fingertip shapes are arbitrary. In this paper, we will tackle this simple problem and show that minimization of such an artifically introduced potential can lead to stable grasping under some good design of fingertip shapes (see Fig. 3).

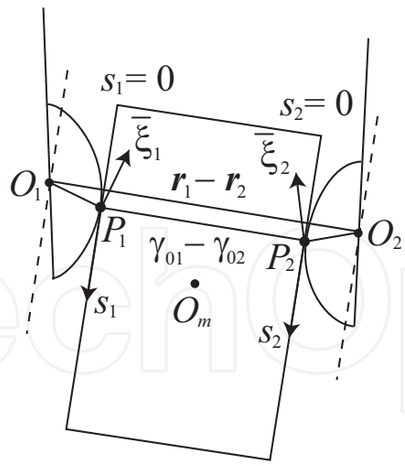

Fig. 3. Minimization of the squared norm $\|\boldsymbol{r}_1 - \boldsymbol{r}_2\|^2$ over rolling motions is attained when the straight line $\overline{P_1P_2}$ connecting the two contact points becomes parallel to the vector $(\boldsymbol{r}_1 - \boldsymbol{r}_2)$, that is, $\overline{O_1O_2}$ becomes parallel to $\overline{P_1P_2}$.

First, we remark that, since the first term of $P(X)$ in (22) in the squared norm of the vector $\overrightarrow{O_2O_1}$ times $\beta/2$, it must be a function only dependent on length parameters s_1 and s_2. Then, it will be shown that minimization of the squared norm $\|\boldsymbol{r}_1 - \boldsymbol{r}_2\|^2$ over rolling contact motions is attained when the straight line $\overline{P_1P_2}$ connecting the two contact points becomes parallel to the vector $(\boldsymbol{r}_1 - \boldsymbol{r}_2)$. That is, $U(X)$ $(= (\beta/2)\|\boldsymbol{r}_1 - \boldsymbol{r}_2\|^2)$ is minimized when $\overline{O_1O_2}$ becomes parallel to $\overline{P_1P_2}$. To show this directly from the set of Euler-Lagrange's equations (1), (2), and (19) seems difficult even in this case. Instead, we remark that $(\boldsymbol{r}_1 - \boldsymbol{r}_2)$ can be expressed in terms of length parameters s_i for $i = 1, 2$ as follows:

$$\boldsymbol{r}_1 - \boldsymbol{r}_2 = -\Pi_1\gamma_1 + \Pi_2\gamma_2 + \Pi_0(\gamma_{01} - \gamma_{02}) \tag{25}$$

where $\Pi_i \in SO(2)$ denotes the rotational matrix of O_i-X_iY_i to be expressed in the frame coordinates O-xy. Since the object is rectangular, all $\boldsymbol{b}_{0i}$ and $\boldsymbol{n}_{0i}$ for $i = 1, 2$ are invariant under the change of s_i for $i = 1, 2$. Therefore, as seen from Fig. 3, if the object width is denoted by l_w and zero points of s_1 and s_2 are set as shown in Fig. 3, then it is possible to write (25) as follows:

$$\boldsymbol{r}_1 - \boldsymbol{r}_2 = (s_1 - s_2)\bar{\boldsymbol{b}}_{01} + (-\boldsymbol{b}_1^{\mathrm{T}}\gamma_1 + \boldsymbol{b}_2^{\mathrm{T}}\gamma_2)\bar{\boldsymbol{b}}_{01} - l_w\bar{\boldsymbol{n}}_{01} + (\boldsymbol{n}_1^{\mathrm{T}}\gamma_1 + \boldsymbol{n}_2^{\mathrm{T}}\gamma_2)\bar{\boldsymbol{n}}_{01} \tag{26}$$

Since $\bar{\boldsymbol{b}}_{01} \perp \bar{\boldsymbol{n}}_{01}$, $U(X)$ can be expressed as

$$\begin{aligned} U(X) &= \frac{\beta}{2}\|\boldsymbol{r}_1 - \boldsymbol{r}_2\|^2 = \frac{\beta}{2}\left\{d^2(s_1, s_2) + l^2(s_1, s_2)\right\} \\ &= U(s_1, s_2) \end{aligned} \tag{27}$$

where

$$d(s_1, s_2) = s_1 - s_2 - \boldsymbol{b}_1^{\mathrm{T}}\gamma_1 + \boldsymbol{b}_2^{\mathrm{T}}\gamma_2 \tag{28}$$

$$l(s_1, s_2) = -l_w + (\boldsymbol{n}_1^{\mathrm{T}}\gamma_1 + \boldsymbol{n}_2^{\mathrm{T}}\gamma_2) \tag{29}$$

Note that the artificial potential $U(X)$ can be regarded as a scalar function defined in terms of length parameters s_1 and s_2. When minimization of $U(s_1, s_2)$ over some parameter intervals

$s_i \in I_i = (a_i, b_i)$ is considered for $i = 1, 2$, it is important to note that the vector $(\boldsymbol{r}_1 - \boldsymbol{r}_2)$ is originally subject to the constraint

$$V(s_1, s_2) = (\boldsymbol{r}_1 - \boldsymbol{r}_2)^{\mathrm{T}} \bar{\boldsymbol{n}}_{01} - \boldsymbol{n}_1^{\mathrm{T}} \gamma_1 - \boldsymbol{n}_2^{\mathrm{T}} \gamma_2 - \boldsymbol{n}_{01}^{\mathrm{T}} \gamma_{01} - \boldsymbol{n}_{02}^{\mathrm{T}} \gamma_{02} = 0 \tag{30}$$

which is obtained by subtraction of Q_{n2} from Q_{n1} defined in (5) and (6). Hence, by introducing a Lagrange multiplier η, minimization of the function

$$W(s_1, s_2; \eta) = U(s_1, s_2) + \eta V(s_1, s_2) \tag{31}$$

must be equivalent to that of $U(X)$. Then it follows that

$$\frac{\partial W}{\partial s_i} = (-1)^i \beta \kappa_i (\boldsymbol{r}_1 - \boldsymbol{r}_2)^{\mathrm{T}} \bar{\boldsymbol{\xi}}_i + \eta \kappa_i \boldsymbol{b}_i^{\mathrm{T}} \gamma_i, \quad i = 1, 2 \tag{32}$$

where we define, for abbreviation,

$$\bar{\boldsymbol{\xi}}_i = (\boldsymbol{n}_i^{\mathrm{T}} \gamma_i) \bar{\boldsymbol{b}}_{0i} + (\boldsymbol{b}_i^{\mathrm{T}} \gamma_i) \bar{\boldsymbol{n}}_{0i}, \quad i = 1, 2 \tag{33}$$

The derivation of this equation is discussed in [Arimoto et al. 2009c]. At this stage, we remark that the vectors $\bar{\boldsymbol{\xi}}_i$ for $i = 1, 2$ appear at contact points P_1 and P_2 as indicated in Fig. 3. Evidently from the right hand side of (32), if we set

$$\eta = \beta (\boldsymbol{r}_1 - \boldsymbol{r}_2)^{\mathrm{T}} \bar{\boldsymbol{n}}_{01} \quad \left(= -\beta (\boldsymbol{r}_1 - \boldsymbol{r}_2)^{\mathrm{T}} \bar{\boldsymbol{n}}_{02} \right) \tag{34}$$

and at the same time

$$(\boldsymbol{r}_1 - \boldsymbol{r}_2)^{\mathrm{T}} \bar{\boldsymbol{b}}_{0i} = 0, \qquad i = 1, 2 \tag{35}$$

then (32) implies

$$\frac{\partial W}{\partial s_i} = 0, \qquad i = 1, 2 \tag{36}$$

In view of the geometrical meaning of (35) that the vector $\overrightarrow{O_2 O_1} \perp \bar{\boldsymbol{b}}_{0i}$, when $\boldsymbol{r}_1 - \boldsymbol{r}_2$ becomes perpendicular to $\boldsymbol{b}_{0i}$ from some starting posture by rolling contact motion, s_i for $i = 1, 2$ must have the same value s^* and $\boldsymbol{b}_1^{\mathrm{T}} \gamma_1 = \boldsymbol{b}_2^{\mathrm{T}} \gamma_2$. That is, satisfaction of the conditions

$$s_1 = s_2 = s^*, \quad \boldsymbol{b}_1^{\mathrm{T}} \gamma_1 = \boldsymbol{b}_2^{\mathrm{T}} \gamma_2 \tag{37}$$

is equivalent to that $\overrightarrow{O_2 O_1}$ becomes parallel to $\overrightarrow{P_2 P_1}$ as shown in Fig. 3. Under (37),

$$\left. \frac{\partial W}{\partial s_i} \right|_{s_i = s^*} = 0, \qquad i = 1, 2 \tag{38}$$

Finally, it is important to check the positivity of the Hessian matrix $H = (\partial^2 U / \partial s_i \partial s_j)$. Bearing in mind the form of (32) together with (34), we obtain [Arimoto et al. 2009c]

$$\begin{aligned} \left. \frac{\partial^2 U}{\partial s_i \partial s_i} \right|_{s_i = s^*} &= \kappa_i (-1)^i \beta (\boldsymbol{r}_1 - \boldsymbol{r}_2)^{\mathrm{T}} \bar{\boldsymbol{n}}_{0i} (\kappa_i \boldsymbol{n}_i^{\mathrm{T}} \gamma_i + \boldsymbol{b}_i^{\mathrm{T}} \gamma_i') \\ &= -\beta l(s_1, s_2) \kappa_i^2 \left(\frac{1}{\kappa_i} + \boldsymbol{n}_i^{\mathrm{T}} \gamma_i \right), \qquad i = 1, 2 \end{aligned} \tag{39}$$

and

$$\left.\frac{\partial^2 U}{\partial s_1 \partial s_2}\right|_{s_i=s^*} = 0 \tag{40}$$

where $l(s_1, s_2)$ is defined by (29). Since $l(s_1, s_2) < 0$ from the geometrical meaning of the situation shown in Fig. 3, it is possible to conclude that the potential function $U(s_1, s_2)$ is minimized at the posture satisfying (37) provided that

$$\frac{1}{\kappa_i(s_i)} > -\boldsymbol{n}_i^{\mathrm{T}}(s_i)\gamma_i(s_i), \qquad i = 1, 2 \tag{41}$$

for all s_i belonging to $(s^* - \delta_i, s^* + \delta_i)$ with some $\delta_i > 0$ for $i = 1, 2$.
Geometric and physical meanings of the condition of (41) will be discussed more in detail in a future paper [Arimoto et al., 2009c].

1.5 Derichlet-Lagrange Stability for Pinching a Rectangular Object

In this section, we show that, when the line connecting the contact points P_1 and P_2 becomes parallel to the line $\overline{O_1O_2}$ as shown in Fig. 3, P(X) is minimized under the constraint of equalities (5) and (6) and at the same time any solution to the set of closed-loop dynamics (1), (2), and (19) under rolling constraints (5) and (6) converges asymptotically to such an equilibrium posture, provided that the solution trajectory starts in a neighborhood of the equilibrium state. To do this, define

$$\begin{cases} \Delta f_i = f_i + \beta l(s_1, s_2) & (42) \\ \Delta\lambda_i = \lambda_i - (-1)^i \beta d(s_1, s_2) & (43) \end{cases}$$

and note that

$$-(-1)^i \beta J_i^{\mathrm{T}}(\boldsymbol{r}_1 - \boldsymbol{r}_2) = \beta J_i^{\mathrm{T}} \left\{ l\bar{\boldsymbol{n}}_{0i} - (-1)^i d\bar{\boldsymbol{b}}_{0i} \right\}, \qquad i = 1, 2 \tag{44}$$

Substituting (44) into (19) and referring to (42) and (43) yield

$$\begin{aligned} G_i\ddot{q}_i + \left\{ \frac{1}{2}\dot{G}_i + S_i \right\} \dot{q}_i + c_i\dot{q}_i + \Delta f_i \left\{ J_i^{\mathrm{T}}\bar{\boldsymbol{n}}_{0i} - (-1)^i(\boldsymbol{b}_i^{\mathrm{T}}\gamma_i)\boldsymbol{e}_i \right\} \\ + \Delta\lambda_i \left\{ J_i^{\mathrm{T}}\bar{\boldsymbol{b}}_{0i} - (-1)^i(\boldsymbol{n}_i^{\mathrm{T}}\gamma_i)\boldsymbol{e}_i \right\} + \Delta N_i \boldsymbol{e}_i = 0, \qquad i = 1, 2 \end{aligned} \tag{45}$$

where

$$\Delta N_i = \beta \left\{ (-1)^i l(\boldsymbol{b}_i^{\mathrm{T}}\gamma_i) - d(\boldsymbol{n}_i^{\mathrm{T}}\gamma_i) \right\} + \alpha_i \{ p_i - p_i(0) \}, \qquad i = 1, 2 \tag{46}$$

On the other hand, (1) and (2) can be rewritten into the forms:

$$M\ddot{\boldsymbol{x}} - \Delta f_1\bar{\boldsymbol{n}}_{01} - \Delta f_2\bar{\boldsymbol{n}}_{02} - \Delta\lambda_1\bar{\boldsymbol{b}}_{01} - \Delta\lambda_2\bar{\boldsymbol{b}}_{02} = 0 \tag{47}$$

$$I\ddot{\theta} - \Delta f_1(\boldsymbol{b}_{01}^{\mathrm{T}}\gamma_{01}) + \Delta f_2(\boldsymbol{b}_{02}^{\mathrm{T}}\gamma_{02}) + \Delta\lambda_1(\boldsymbol{n}_{01}^{\mathrm{T}}\gamma_{01}) - \Delta\lambda_2(\boldsymbol{n}_{02}^{\mathrm{T}}\gamma_{02}) + S_N = 0 \tag{48}$$

where

$$S_N = \beta l(\boldsymbol{b}_{01}^{\mathrm{T}}\gamma_{01} - \boldsymbol{b}_{02}^{\mathrm{T}}\gamma_{02}) - \beta d(\boldsymbol{n}_{01}^{\mathrm{T}}\gamma_{01} + \boldsymbol{n}_{02}^{\mathrm{T}}\gamma_{02}) = \beta \{ (s_1 - s_2)l + l_w d \} \tag{49}$$

Now it is possible to show that the set of equations (47) to (49) together with (7) can be regarded as a set of Euler-Lagrange equations obtained by applying the variational principle to the Lagrangian

$$L = K(X, \dot{X}) - U(s_1, s_2) + \sum_{i=1,2} (\Delta f_i Q_{ni} + \Delta\lambda_i Q_{bi}) \tag{50}$$

in which the external forces of damping $c_i\dot{q}_i$ for $i = 1, 2$ through finger joints are taken into account. In fact, from (27) to (29) it follows that

$$\begin{aligned} \frac{\mathrm{d}U(s_1, s_2)}{\mathrm{d}t} &= \sum_{i=1,2} \frac{\mathrm{d}U_i}{\mathrm{d}s_i}\frac{\mathrm{d}s_i}{\mathrm{d}t} = \sum_{i=1,2} (-1)^i \beta \left\{ (\boldsymbol{n}_i^{\mathrm{T}}\gamma_i)d - (-1)^i(\boldsymbol{b}_i^{\mathrm{T}}\gamma_i)l \right\} \kappa_i \frac{\mathrm{d}s_i}{\mathrm{d}t} \\ &= \sum_{i=1,2} \beta \left\{ (\boldsymbol{n}_i^{\mathrm{T}}\gamma_i)d - (-1)^i(\boldsymbol{b}_i^{\mathrm{T}}\gamma_i)l \right\} (\dot{\theta} - \dot{p}_i) \qquad (51) \\ &= \beta \left\{ \boldsymbol{n}_1^{\mathrm{T}}\gamma_1 + \boldsymbol{n}_2^{\mathrm{T}}\gamma_2)d + (\boldsymbol{b}_1^{\mathrm{T}}\gamma_1 - \boldsymbol{b}_2^{\mathrm{T}}\gamma_2)l \right\} \dot{\theta} + \sum_{i=1,2} \beta N_i \dot{p}_i \qquad (52) \end{aligned}$$

where N_i is defined as

$$N_i = (-1)^i(\boldsymbol{b}_i^{\mathrm{T}}\gamma_i)l - (\boldsymbol{n}_i^{\mathrm{T}}\gamma_i)d \tag{53}$$

By using (28) and (29), (52) can be written as

$$\begin{aligned} \frac{\mathrm{d}U(s_1, s_2)}{\mathrm{d}t} &= \beta \left\{ (l + l_w)d + (s_1 - s_2 - d)l \right\} \dot{\theta} + \sum_{i=1,2} \beta N_i \dot{p}_i \\ &= S_N\dot{\theta} + \sum_{i=1,2} \beta N_i \boldsymbol{e}_i^{\mathrm{T}} \dot{q}_i \qquad (54) \end{aligned}$$

Thus, we conclude that from (46) the variation of P takes the form

$$\begin{aligned} dP &= d\left[U + \sum \frac{\alpha_i}{2} \left\{ p_i - p_i(0) \right\}^2 \right] \\ &= S_N d\theta + \sum_{i=1,2} \left[\beta N_i + \alpha_i \left\{ p_i - p_i(0) \right\} \right] \mathrm{d}p_i \\ &= S_N d\theta + \sum_{i=1,2} \Delta N_i \boldsymbol{e}_i^{\mathrm{T}} \mathrm{d}q_i \qquad (55) \end{aligned}$$

The last term of the left hand side of (48) comes directly from the first term of the right hand side of (55) in the variational form of the potential $P(X, s_1, s_2)$. The last term $\Delta N_i \boldsymbol{e}_i$ also comes directly from the last term of (55). Thus, it is possible to prove that, if the posture of the fingers-object system satisfying the condition that $\overline{O_1O_2}$ is parallel to $\overline{P_1P_2}$ as shown in Fig. 3 is an isolated equilibrium state, then the posture must be asymptotically stable because the system is fully dissipated (see [Arimoto, 2010]), no matter how the system is holonomically constrained. If both the fingers are of single degrees-of-freedom, then the total degrees-of-freedom of the system becomes single and therefore the equilibrium state is isolated. In a case of redundant degrees-of-freedom system like the setup illustrated in Fig. 1, it is necessary to extend the so-called Dirichlet-Lagrange stability theorem (see [Arimoto et al., 2009c] and [Arimoto, 2010a]) to a system with redundancy in degree-of-freedom together with holonomic constraints. Such an extension of the theorem is possible as already discussed in a special class of robot control problems (see [Arimoto, 2007]), but the details are too mathematically sophysticated and therefore will be discussed in a future paper.

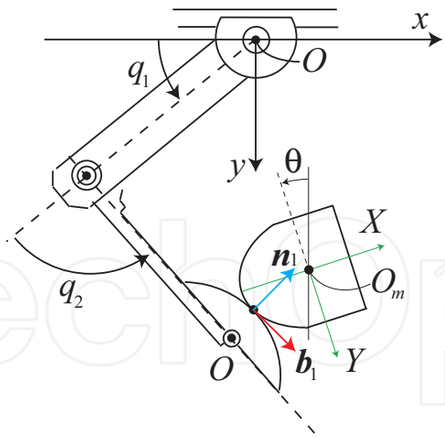

Fig. 4. Robot finger pinching an object pivoted at a fixed point O_m.

1.6 Conclusions

Modeling and control of precision prehension of 2-D objects by a pair of planar robot fingers with an arbitrary fingertip geometry are discussed. Stability of a control signal based upon the fingers-thumb opposition is analyzed by extending the Dirichlet-Lagrange stability theorem in a case that the object has parallel flat surfaces.

To find an effective control scheme that stabilizes grasping of an object with an arbitrary geometry remains unsolved, even in the case of 2-D grasping.

2. Simulation of 2-D Grasping under Physical Interaction of Rolling between Arbitrary Smooth Contour Curves

2.1 Introduction

Numerical simulation of motions of a rolling contact between two 2-dimensional (2-D) rigid bodies with an arbitrary smooth contour is carried out by using an extended constraint stabilization method (CSM), in order to testify the physical validity of the Euler-Lagrange equation of rolling contact motion. To gain a physical insight into the problem, a simpler control problem is treated in relation to stabilization of a rotational motion of a rigid body pivoted around a fixed point in a horizontal plane by using a planar robot with two joints. A CSM is applied extensively to the derived Euler-Lagrange equation that is characterized by an arclength parameter, that is commonly used to specify the contact position on the object contour and the fingertip contour. In parallel to the Euler-Lagrange equation, a first-order differential equation of the arclength parameter must be integrated simultaneously in order to update the position of the rolling contact (see [Yoshida et al., 2009a and 2009b]).

2.2 A Testbed Problem of Stabilization for Rolling Contact Motion

In order to gain a physical and intuitive insight into a rolling contact phenomenon between two rigid bodies in a horizontal plane, a simple mechanical setup depicted in Fig. 4 is considered. The robot finger has two joints and its fingertip is shaped by an arbitrary smooth contour curve. The object pivots around the fixed point O_m $(= (x, y))$ and has a contour with an arbitrary geometry. It is assumed that motion of the overall fingers-object system is restricted to the horizontal plane and therefore the effect of gravity is ignored. Denote the joint vector of

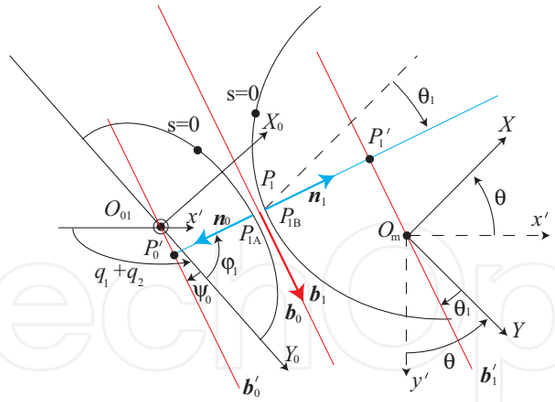

Fig. 5. Geometrical relationship between local coordinates O_m-XY and O_{01}-X_0Y_0.

finger joint angles by $q = (q_1, q_2)^{\mathrm{T}}$ and the orientation angle of the object by θ. As shown in Fig. 4, O-xy expresses the inertial frame, O_m-XY the local coordinates attached to the object, and O_{01}-X_1Y_1 the local coordinates of the fingertip as shown in Fig. 5. Suppose that the object contour is described by a curve $\gamma(s) = (X(s), Y(s))^{\mathrm{T}}$ with the aid of the arclength parameter s as shown in Fig. 4 and Fig. 5. At the same time, define the unit tangent $\boldsymbol{b}_1(s)$ and the unit normal $\boldsymbol{n}_1(s)$ at the contact point P_{1B} as shown in Fig. 5. Similarly, define $\boldsymbol{b}_0(s)$ and $\boldsymbol{n}_0(s)$ at the contact point P_{1A} on the contour curve $\gamma_0(s) = (X_0(s), Y_0(s))$ of the fingertip. Since we assume that the two contact points P_{1A} and P_{1B} must coincide at a single common point P_1 without mutual penetration and the two contours share the same tangent at the contact point, $\boldsymbol{n}_0 = -\boldsymbol{n}_1$ and $\boldsymbol{b}_0 = \boldsymbol{b}_1$ as seen in Fig. 5. If we define angles $\theta_1(s)$ and $\psi_0(s)$ by

$$\theta_1(s) = \arctan\{X'(s)/Y'(s)\} \tag{56}$$

$$\psi_0(s) = \arctan\{X_0'(s)/Y_0'(s)\} \tag{57}$$

then unit tangents and normals can be expressed as

$$\boldsymbol{b}_1 = \begin{pmatrix} \sin(\theta+\theta_1) \\ \cos(\theta+\theta_1) \end{pmatrix}, \quad \boldsymbol{b}_0 = \begin{pmatrix} -\cos(q_1+q_2+\psi_0) \\ \sin(q_1+q_2+\psi_0) \end{pmatrix} \tag{58}$$

$$\boldsymbol{n}_1 = \begin{pmatrix} \cos(\theta+\theta_1) \\ -\sin(\theta+\theta_1) \end{pmatrix}, \quad \boldsymbol{n}_0 = -\begin{pmatrix} \sin(q_1+q_2+\psi_0) \\ \cos(q_1+q_2+\psi_0) \end{pmatrix} \tag{59}$$

where we denote the derivative of $X(s)$ in s by $X'(s)$ $(= \mathrm{d}X(s)/\mathrm{d}s)$ and similarly the derivatives of $Y(s)$, $X_0(s)$, and $Y_0(s)$ by $Y'(s)$, $X_0'(s)$, and $Y_0'(s)$. Further, it is important to introduce the following four quantities that can be determined from the local fingertip and object geometries (see Fig. 6):

$$l_{b0}(s) = X_0(s)\sin\psi_0 + Y_0(s)\cos\psi_0 \tag{60}$$

$$l_{b1}(s) = -X(s)\sin\theta_1 - Y(s)\cos\theta_1 \tag{61}$$

$$l_{n0}(s) = X_0(s)\cos\psi_0 - Y_0(s)\sin\psi_0 \tag{62}$$

$$l_{n1}(s) = -X(s)\cos\theta_1 + Y(s)\sin\theta_1 \tag{63}$$

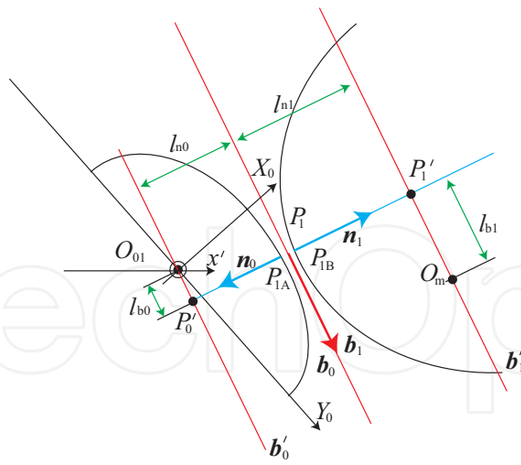

Fig. 6. Geometrical relationship of l_{n0}, l_{n1}, l_{b0}, and l_{b1}.

As discussed in detail by [Arimoto et al., 2009a], the rolling contact constraint is composed of the two algebraic equations:

$$R = (x_{01} - x)\sin(\theta + \theta_1) + (y_{01} - y)\cos(\theta + \theta_1) + l_{b0}(s) + l_{b1}(s) = 0 \tag{64}$$

$$Q = (x_{01} - x)\cos(\theta + \theta_1) - (y_{01} - y)\sin(\theta + \theta_1) + l_{n0}(s) + l_{n1}(s) = 0 \tag{65}$$

Note that these two equalities express the geometrical relations described in the following ways (see Fig. 6):

$$\overline{P_0'P_1'} = l_{no} + l_{n1} \tag{66}$$

$$\overline{O_m P_1'} + \overline{P_0' O_{01}} = l_{b0} + l_{b1} \tag{67}$$

Further, from the definition of directional derivatives of $\boldsymbol{b}_0$ and $\boldsymbol{b}_1$ that coincide at the contact point, the arclength parameter should be updated through the following first-order differential equation [Arimoto et al., 2009a]:

$$\{\kappa_0(s) + \kappa_1(s)\}\frac{\mathrm{d}s}{\mathrm{d}t} = (\dot{q}_1 + \dot{q}_2 - \dot{\theta}) \tag{68}$$

where $\kappa_0(s)$ denotes the curvature of the fingertip contour curve and $\kappa_1(s)$ that of the object contour. These quantities can be calculated from the quantities of the second fundamental form as follows:

$$\kappa_0(s) = -X_0''(s)Y_0(s) + X_0'(s)Y_0''(s) \tag{69}$$

$$\kappa_1(s) = X''(s)Y'(s) - X'(s)Y''(s) \tag{70}$$

The total kinetic energy of the system is given by the form

$$K = \frac{1}{2}\dot{q}^{\mathrm{T}} G(q)\dot{q} + \frac{1}{2} I\dot{\theta}^2 \tag{71}$$

where $G(q)$ stands for the inertia matrix of the finger and I for the inertia moment of the object rigid body around the pivotal axis at O_m. Then, by applying the variational principle for the Lagrangian

$$L = K - fQ - \lambda R \tag{72}$$

the following Euler-Lagrange equation is obtained [Arimoto et al., 2009a]:

$$I\ddot{\theta} + fl_{b1} - \lambda l_{n1} = 0 \tag{73}$$

$$G(q)\ddot{q} + \left\{\frac{1}{2}\dot{G}(q) + S(q,\dot{q})\right\}\dot{q} + f\{J_{01}^{\mathrm{T}}(q)\boldsymbol{n}_1 + l_{b0}\boldsymbol{e}\} + \lambda\{J_{01}^{\mathrm{T}}(q)\boldsymbol{b}_1 - l_{n0}\boldsymbol{e}\} = u \tag{74}$$

where $\boldsymbol{e} = (1,1)^{\mathrm{T}}$ and f and λ signify Lagrange's multipliers corresponding to constraints $Q = 0$ and $R = 0$ respectively. Finally, we introduce the control signal

$$u = -c\dot{q} - \frac{f_d}{r}J_{01}^{\mathrm{T}}(q)\begin{pmatrix} x_{01} - x \\ y_{01} - y \end{pmatrix} \tag{75}$$

where c stands for a positive damping constant and f_d/r a positive constant with the physical dimension [N/m]. It should be noted [Arimoto et al., 2009a] that by substituting u of (75) into (74) and rewriting (73) and (74), we obtain the closed-loop dynamics of the system described by

$$I\ddot{\theta} + \Delta f\frac{\partial Q}{\partial\theta} + \Delta\lambda\frac{\partial R}{\partial\theta} + \frac{f_d}{r}N_1 = 0 \tag{76}$$

$$G(q)\ddot{q} + \left\{\frac{1}{2}\dot{G} + S\right\}c\dot{q} + \Delta f\frac{\partial Q}{\partial q} + \Delta\lambda\frac{\partial R}{\partial q} - \frac{f_d}{r}N_1\boldsymbol{e} = 0 \tag{77}$$

where

$$\begin{cases} \Delta f = f + \dfrac{f_d}{r}Q_1, \quad \Delta\lambda = \lambda + \dfrac{f_d}{r}R_1 \\ N_1 = l_{b0}Q_1 - l_{n0}R_1 = -l_{b0}l_{n1} + l_{n0}l_{b1} \end{cases} \tag{78}$$

and

$$Q_1 = -l_{n0}(s) - l_{n1}(s), \quad R_1 = l_{b0}(s) + l_{b1}(s) \tag{79}$$

2.3 Numerical Simulation

We carry out numerical simulations in order to verify the validity of the derived mathematical model and the effectiveness of the control signal. The physical parameters of the overall system are given in Table 1 and the control input parameters are in Table 2. As an object with an arbitrary geometry, the contour carve $\gamma(s) = (X(s), Y(s))$ is given by a function described by

$$X(s) = -0.03 + \frac{\sqrt{1 + 4 \times 50^2 \times (s - 3.363 \times 10^{-3})^2}}{2 \times 50} \tag{80}$$

$$Y(s) = \frac{A\,\sinh(2 \times 50 \times (2 - 3.363 \times 10^{-3}))}{2 \times 50} \tag{81}$$

The fingertip contour curve is given by a function described as

$$X_0(s) = 0.035 - \frac{\sqrt{1 + 4 \times 20^2 \times s}}{2 \times 20} \tag{82}$$

$$Y_0(s) = \frac{A\,\sinh(2 \times 20 \times s)}{2 \times 20} \tag{83}$$

l_{11}	length	0.065 [m]
l_{12}	length	0.065 [m]
m_{11}	weight	0.045 [kg]
m_{12}	weight	0.040 [kg]
I	object inertia moment	6.6178×10^{-6} [kgm^2]

Table 1. Physical parameters of the fingers and object.

f_d	internal force	0.500 [N]
c	damping coefficient	0.006 [Nms]
r	constant value	0.010 [m]
γ_{f1}	CSM gain	1500
$\gamma_{\lambda 1}$	CSM gain	3000
ω_{f1}	CSM gain	225.0×10^4
$\omega_{\lambda 1}$	CSM gain	900.0×10^4

Table 2. Parameters of control signals & CSM gains.

Both the contour curves are depicted in Fig. 7. The pair of the second-order differentia equations (73) and (74) together with (75) and the other pair of holonomic constraints expressed by (64) and (65) are combined into a CSM form by introducing a pair of CSM gains γ_{f1} and ω_{f1} and another pair of $\gamma_{\lambda 1}$ and $\omega_{\lambda 1}$ that are given in Table 2. In the CSM form, the derivative of length parameter s in t is required, which is obtained by the update equation of the length parameter shown in (68). As discussed in the recent paper [Arimoto et al., 2009b], the equilibrium sate is realized when the line $\overline{O_{01}O_m}$ meets the contact point P_1. In other words, the artificial potential $U(s) = \frac{f_d}{2r}\{(l_{b1}+l_{b0})^2 + (l_{n0}+l_{n1})^2\}$ is minimized at the position satisfying $N_1 = 0$, that is, the line $\overline{O_{01}O_m}$ meets the contact point P_1.
We show the initial pose of the system and another pose of the system after 3.0 [s] in Fig. 8. The initial pose is obtained by solving the inverse kinematics problem and the initial angular velocities $\dot{q}_i$ $(i = 1, 2)$ and $\dot{\theta}$ are set zero in this simulation. The trasient responses of all physical variables are shown in Figs. 9 to 17. As seen from Fig. 11, N_1 tends to zero as t increases and, in parallel to this fact, the value of the artificial potential $U(s)$ tends to its minimum as t increases as shown in Fig. 18. As predicted from Fig. 8 (b), the system's position tends to converge to the posture at which the line connecting the fingertip center O and the object center O_m meets the contact point P_1.

2.4 Conclusions

A preliminary result of numerical simulation of control of rolling contact motions between two 2-D rigid bodies with an arbitrary contour curve is presented. In this note, the two contour curves are given in an analytically well-defined form. Nevertheless, to construct a numerical simulator for the purpose of its preactical use, it is necessary to design another numerical simulator that can calculate numerical quantities of the second fundamental form when the concerned contour curves are given by a set of numerical data points. Then, the problem for finding a unique contact point between the two contour curves without penetration becomes crucial in the design of such a practically useful simulator.

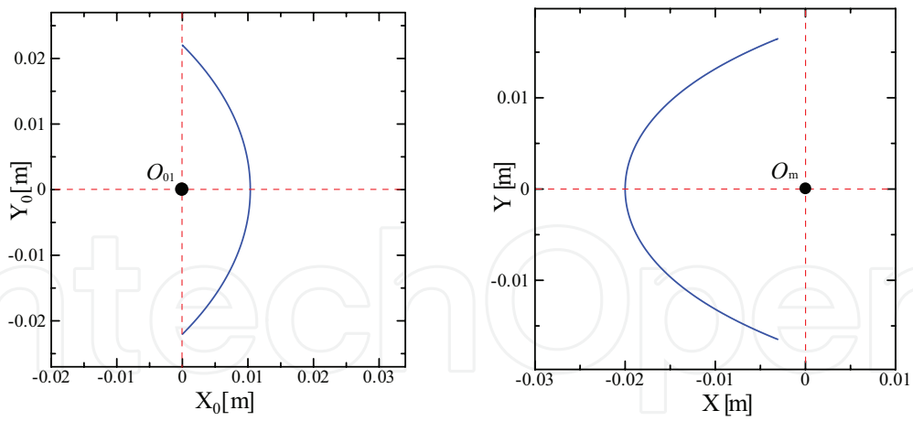

(a) The curve of the fingertip's contour (b) The curve of the object's contour

Fig. 7. The local coordinates of the fingertip and the object.

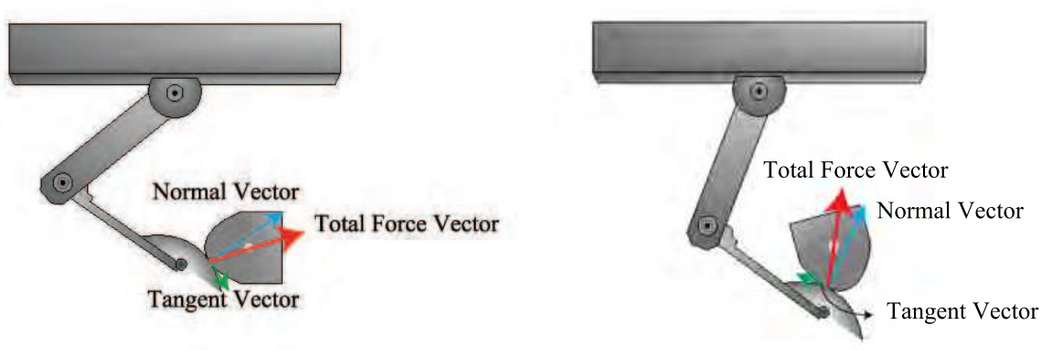

(a) Initial pose (b) After 3 seconds

Fig. 8. Motion of pinching a 2-D object with arbitrary shape.

3. Modeling of 3-D Grasping under Rolling Contacts between Arbitrary Smooth Surfaces

3.1 Introduction

A possible extension of modeling and control of 2-D (2-dimensional) grasping of a rigid object by means of a pair of planar robot fingers to 3-D grasping under rolling contacts is discussed, under the circumstance of an arbitrary geometry of surfaces of the robot fingertips and a given 3-D rigid object.

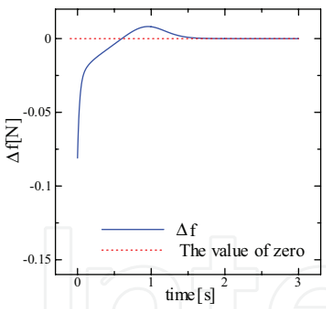

Fig. 9. Δf

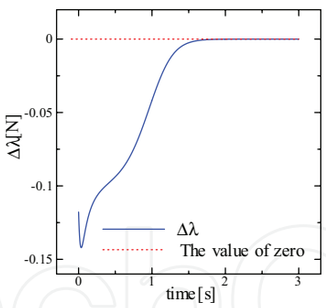

Fig. 10. $\Delta\lambda$

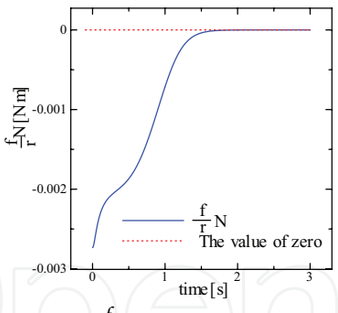

Fig. 11. $\frac{f_d}{r}N_1$

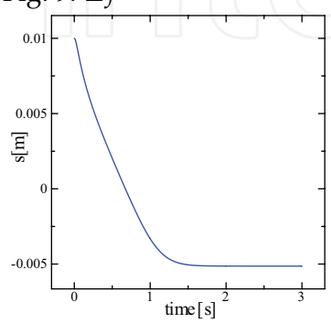

Fig. 12. s

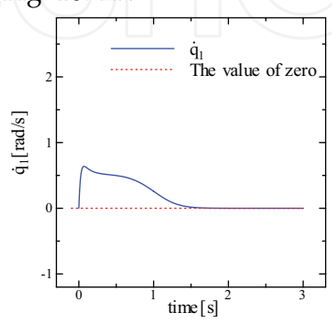

Fig. 13. $\dot{q}_1$

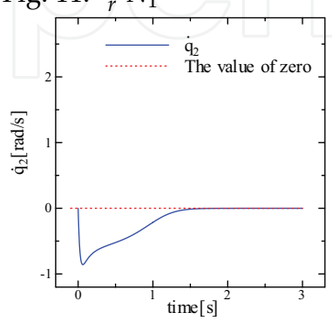

Fig. 14. $\dot{q}_2$

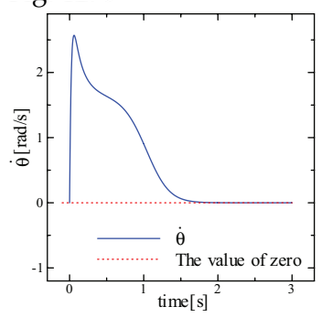

Fig. 15. $\dot{\theta}$

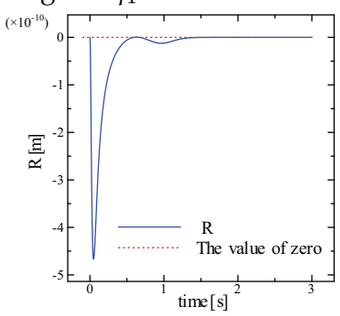

Fig. 16. R

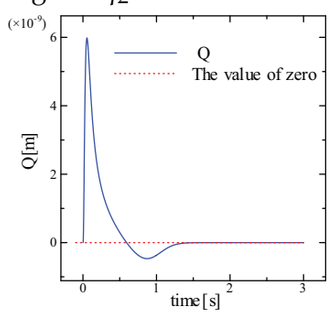

Fig. 17. Q

3.2 Mathematical Modeling of 3-D Grasping under Rolling Contacts

Very recently in the previous papers [Arimoto et al., 2009a and 2009b], a complete set of Euler-Lagrange equations of motion of 2-dimensional grasping under rolling contact constraints is given in a wrench space form from the standpoint of a new definition of rolling contact constraints. The rolling contact between two rigid bodies with smooth surfaces is now interpreted as a condition that the contact points coincide at a single point and share a common tangent at the contact point. This standpoint was first proposed in differential geometry by Nomizu [Nomizu, 1978], that reflects in a two-dimensional case a well-known theorem on curves that, given two smooth planar curves with the same curvature along their arclengths respectively, the one can coincide with another by a homogeneous transformation. The recent works [Arimoto et al., 2009a and 2009b] show that such a mathematical observation can be extended more to the dynamics and control of physical interaction between 2-D rigid bodies with an arbitrary geometry.

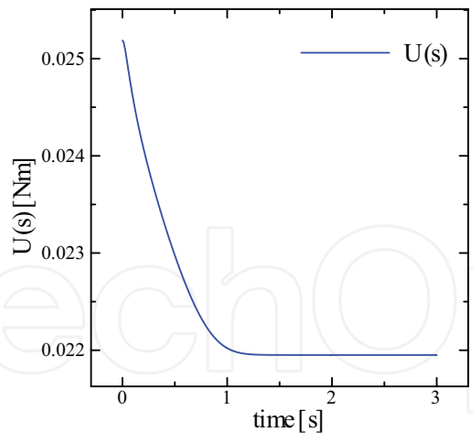

Fig. 18. Transient responses of the value of $U(s(t))$.

This note is concerned with a certain possibility of extending this standpoint to the problem of modeling and control of 3-D grasping under rolling contact constraints (see Fig. 19). Fortunately, it is also well-known in geometry of curves and surfaces that, given two smooth curves in the 3-D Enclidean space characterized by the common arclength parameters, the curves can coincide by finding an adequate homogeneous transformation if and only if the curves have the same curvature and torsion along their arclength parameters. Again in the work [Nomizu, 1978], Nomizu showed a mathematical model of rolling an n-D submanifold M on another n-D submanifold N in a Euclidean space and obtained a kinematic interpretation of the second fundamental form. Thus, we observe that, even in the case of 3-D motion of rolling contacts, each locus of points of the contact between the two surfaces can be characterized by a curve $\gamma_i(s)$ lying on each corresponding surface S_i (see Fig. 20). Thus, a rolling contact as a physical interaction of a rigid object with a rigid fingertip is interpreted by the following two conditions:
A-1) Given a curve $\gamma_1(s_1)$ as a locus of points of the contact on S_1 and another curve $\gamma_0(s_0)$ as a locus of contact points on S_0, the two curves coincide at contact point P_1 and share the same tangent plane at P_1 (see Fig. 20).
A-2) During any continuation of rolling contact, the two curves $\gamma_0(s_0)$ and $\gamma_1(s_1)$ can be described in terms of the same length parameter s in such a way that $s_0 = s + c_0$ and $s_1 = s + c_1$, where c_0 and c_1 are constant.
The details of derivation of the Euler-Lagrange equation of grasping motion of the fingers-object system will be presented in the paper [Arimoto, 2010b].

3.3 Computational Backgrounds for Design of a Numerical Simulator

In the case of 3-D grasping, the core of a numerical simulator for numerically evaluating the loci of contact points between the rigid bodies must be an algorithmic tool for determining the unique contact point together with finding the common tangent and the normal to the tangent between the two surfaces whose data are given as a huge amount of data points. A common contact point should be uniquely determined from the set of data points without penetrating through each other, in conjunction with finding the common tangent and normal at the contact point. Numerical evaluation of the normal curvatures along the loci $\gamma_i(s)$ on the surfaces is also indispensable for contruction of a numerical simulator. Once the numerical data of all

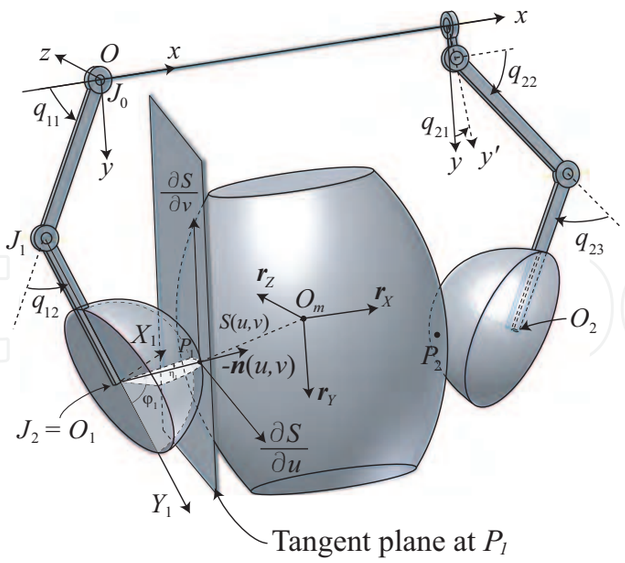

Fig. 19. A pair of robot fingers is grasping a rigid object with arbitrary smooth surfaces. The inertial frame is denoted by the coordinates O-xyz and the body coordinates are expressed by O_m-XYZ with body-fixed unit vectors $\boldsymbol{r}_X$, $\boldsymbol{r}_Y$, and $\boldsymbol{r}_Z$.

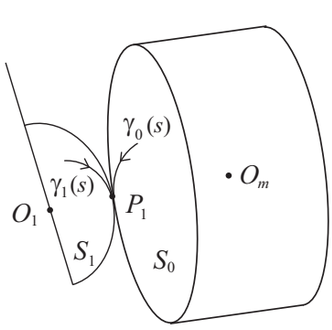

Fig. 20. A locus of points of contact on the left hand fingerend surface S_1 is denoted by $\gamma_1(s)$ and that on the object surface by $\gamma_0(s)$. If there does not arise any slipping, both loci can be traced by the common length parameter s.

the loci $\gamma_i(s)$ are calculated through the Euler-Lagrange equation, all the geometrical data of motion of the robot fingers and the object can be recovered from the kinematics and the equalities of rolling contact constraints. Then, visualization is a matter of course of computer graphics of curves and surfaces.

4. References

Arimoto, S.; Yoshida, M.; Sekimoto, M; Tahara, K. (2009a). Modeling and control of 2-D grasping of an object with arbitrary shape under rolling contact, *SICE J. of Control, Measurement and System Integration*, Vol. 2, No. 6, pp. 379-386

Arimoto, S.; Yoshida, M.; Sekimoto, M.; Tahara, K. (2009b). A Riemannian-geometry approach for control of robotic systems under constraints, *SICE J. of Control, Measurement and System Integration*, Vol. 2, No. 2, pp. 107–116

Nomizu, K. (1978). *Kinematics and differential geometry of submanifolds – Rolling a ball with a prescribed locus of contact –*, Tohoku Math. Journ., Vol. 30, pp. 623–637

Gray, A.; Abbena, E.; Salamon, S. (2006). *Modern Differential Geometry of Curves and Surfaces with Mathematica*, Chapman & Hall/CRC, Boca Raton, Florida, USA

Arimoto, S. (2008). *Control Theory of Multi-fingered Hands: A Modelling and Analytical-Mechanics Approach for Dexterity and Intelligence*, Springer, London, Great Britain

Arimoto, S.; Yoshida, M.; Sekimoto, M.; Bae, J.-H. (2009c). A Riemannian-geometric approach for intelligent control of multi-fingered hands, submitted to *Advanced Robotics* in August 2009 and accepted for publication in October 2009

Arimoto, S. (2010a). Derichlet-Lagrange stability for redundant mechanical systems under constraints: A Riemannian geometric approach for Bernstein's problem of degrees-of-freedom, to be submitted to *SICE J. of Control, Measurement and System Integration*

Arimoto, S. (2007). A differential-geometric approach for 2D and 3D object grasping and manipulation, *Annual Review in Control*, Vol. 31, No. 2, pp. 189–209

Yoshida, M.; Arimoto, S.; Tahara, K. (2009a). Manipulation of 2D object with arbitrary shape by robot finger under rolling constraint, *Proc. of the ICROS-SICE Int. Conf. 2009*, Fukuoka, Japan, August 18-21, pp. 695–699

Yoshida, M.; Arimoto, S.; Tahara, K. (2009b). Pinching 2D object with arbitrary shape by two robot fingers under rolling constraints, to be published in *Proc. of the IROS 2009*, Saint Louis, USA, Oct. 11-15, pp. 1805-1810

Arimoto, S. (2010b). Dynamics of grasping a rigid object with arbitrary smooth surfaces under rolling contacts, *SICE J. of Control, Measurement and System Integration*, to be published in Vol. 3

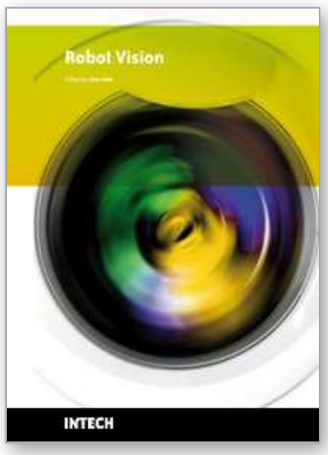

Robot Vision

Edited by Ales Ude

ISBN 978-953-307-077-3
Hard cover, 614 pages
Publisher InTech
Published online 01, March, 2010
Published in print edition March, 2010

The purpose of robot vision is to enable robots to perceive the external world in order to perform a large range of tasks such as navigation, visual servoing for object tracking and manipulation, object recognition and categorization, surveillance, and higher-level decision-making. Among different perceptual modalities, vision is arguably the most important one. It is therefore an essential building block of a cognitive robot. This book presents a snapshot of the wide variety of work in robot vision that is currently going on in different parts of the world.

How to reference

In order to correctly reference this scholarly work, feel free to copy and paste the following:

Suguru Arimoto, Morio Yoshida, and Masahiro Sekimoto (2010). Computational Modeling, Visualization, and Control of 2-D and 3-D Grasping under Rolling Contacts, Robot Vision, Ales Ude (Ed.), ISBN: 978-953-307-077-3, InTech, Available from: http://www.intechopen.com/books/robot-vision/computational-modeling-visualization-and-control-of-2-d-and-3-d-grasping-under-rolling-contacts

INTECH
open science | open minds

InTech Europe
University Campus STeP Ri
Slavka Krautzeka 83/A
51000 Rijeka, Croatia
Phone: +385 (51) 770 447
Fax: +385 (51) 686 166
www.intechopen.com

InTech China
Unit 405, Office Block, Hotel Equatorial Shanghai
No.65, Yan An Road (West), Shanghai, 200040, China
中国上海市延安西路65号上海国际贵都大饭店办公楼405单元
Phone: +86-21-62489820
Fax: +86-21-62489821

IntechOpen